INVESTIGATION OF EARTHQUAKE DISPLAY IN EM FIELD AND IONOSPHERE

Vasily Yu. Belashov[1], Oleg A. Kharshiladze[2]

[1]*Institute of Physics, Kazan Federal University, Kazan, Russia*
[2]*Iv. Javaxishvilis Tbilisi State University, Tbilisi, Georgia*

In this paper we present the results of our investigation of displaying of seismic activity in variations of both the electromagnetic (EM) field and the basic ionospheric characteristics. The 3D case is considered taking into account the effects of weak nonlinearity, dispersion and dissipation in medium, that allows us to obtain more accurate results for both the near and far zones from the earthquake epicenter. In study of the seismic response in the EM field, it is shown that a precursor arises ahead the front of seismic wave, its amplitude decreases exponentially with distance. In case of a single compression pulse, the precursor is negative, and its amplitude depends on the medium conductivity and the parameters of the wave. With increasing conductivity, the amplitude of precursor increases, and its characteristic scale decreases. Regarding the response at ionospheric heights, the seismo-ionospheric post-effects have been studied, which are of great interest, in particular, for a better understanding of relationships in the system "solid Earth – atmosphere – ionosphere" and for identification of seismically caused oscillations in the spectrum of the ionospheric fluctuations, etc. The effect of the acoustic impulse caused by the Rayleigh wave on the ionosphere's neutral component near the epicenter is considered, and further formation of the solitary IGWs and the TIDs, which are caused by them, at the *F*-layer heights in the far zone. The results obtained are in good agreement with the results of our radiophysical experiments during seismic events at the Russia Far East region.

Keywords: ionosphere, electromagnetic field, earthquake, precursor, Rayleigh wave, IGW and TID solitons.

1. Introduction

A number of experimental works starting from the 70s of the last century (see, e.g., [1-3] and rather complete review [4]) reported the observation of low-frequency perturbations of the Earth's electromagnetic (EM) field a few seconds or minutes before the appearance of a seismic wave at a registration point. As possible reasons for this phenomenon, an assumption was made about the excitation in the *E*-layer of the ionosphere during an earthquake of a low-frequency whistler propagating horizontally with a velocity of ~ 20 km/s or slightly slower (10 km/s and lower [4]). Another possible physical mechanism of the phenomenon is associated with the manifestation of the induction seismomagnetic effect in the earth's crust. In theoretical papers [5, 6] it was shown that both in the region of the medium's motion and in front of

the front of the seismic wave, a system of currents and fields perturbing the Earth's EM field appears. Geomagnetic disturbances ahead of the seismic wave will be called EM precursors. Such a precursor was interpreted in [7] as an analogue of Cherenkov radiation in a conducting medium. Studies conducted in [8], however, show that this phenomenon is described by non-wave equations that do not allow such an interpretation. In Sect. 2 we, following mainly the ideology proposed in [8] and developed in [4], show that EM precursors are diffusive in nature, and we also obtain simple laws that determine the spatial size, characteristic duration and amplitude of the precursor.

It is necessary to note that the seismic effects are displayed not only in the solid crust of the Earth, but also at heights of the ionosphere of the Earth. The issues of studying these effects in the ionospheric plasma caused by seismic phenomena are currently attracting the attention of researchers in connection with the importance of this problem not only for "pure" science, but also for ensuring the safe life of the population in seismically dangerous regions and on the planet as a whole. At the same time, along with the study of seismo-ionospheric phenomena – predictors of seismic activity, an important role is played by the study of seismo-ionospheric post-effects, for example, to better understand cause-effect relationships in the system "solid Earth – atmosphere – ionosphere", for bearing of earthquake epicenters, allocation of seismically caused oscillations in the spectrum of ionospheric fluctuations, etc.

As it is known, one of the first attempts at a rather rigorous theoretical study of seismo-ionospheric effects caused by a surface Rayleigh wave was made in [9], where authors used the one-dimensional (1D) linear non-dissipative approximation to solve this problem. A similar approach, taking into account losses caused by the weak electrical conductivity of the medium, was taken in [10]. The influence of weak nonlinearity on the propagation in the ionosphere of an acoustic pulse caused by an earthquake was studied in [11], however, only the 1D case was also considered there. The 3D nonstationary problem of seismic influence on the ionospheric plasma was considered in [12], however, in this study the authors neglected nonlinear effects. Thus, all the studies known (see rather full our review in [4]) had one or another disadvantages and, therefore, the estimates of influence of seismic events on the dynamics of the ionospheric plasma obtained in them turned out to be very approximate. Thus, all the studies known have one or another disadvantages and, therefore, the estimates of influence of seismic events on the dynamics of the ionospheric plasma obtained in them are very approximate. More accurate results can be obtained by taking into account all significant factors. A good example of this approach, in comparison with previous results [10], is the theoretical estimates obtained in [13, 14] for the internal gravitational waves (IGWs) excited by the Rayleigh wave. Sect. 3 presents the results of a theoretical study of the problem, taking into account weak nonlinearity and dispersion, the influence of dissipation and stochastic fluctuations of the electron density, which take place in the ionosphere, in 3D geometry.

2. Seismo-Electromagnetic Effects

Let us consider a conducting homogeneous medium with a constant coefficient of electrical conductivity σ located in a uniform magnetic field with induction $\mathbf{B}_0$. At time $t = 0$, a spherically symmetric acoustic longitudinal wave arises in the medium. The quasistationary Maxwell equations describing the EM disturbances **B**, **E** ($B << B_0$) have form

$$\partial_t \mathbf{B} = D\Delta\mathbf{B} + \mathrm{rot}\left[\mathbf{v},\mathbf{B}_0\right], \qquad \mu_0\,\mathrm{rot}\mathbf{B} = \sigma\left(\mathbf{E} + \left[\mathbf{v},\mathbf{B}_0\right]\right), \tag{1}$$

where $\mathbf{v} = v(r,t)\mathbf{e}_r$ is the preset velocity field, $D = (\mu_0\sigma)^{-1}$ is the magnetic viscosity having the dimension of the diffusion coefficient. We choose the spherical coordinate system (r, θ, φ) with the reference point at the center of symmetry. Then only three components of the field, B_r, B_θ, E_φ, which depend on the variables r, θ, t, will be nonzero. The solution to such a problem with zero initial conditions and the requirement of boundedness of all functions at zero and at infinity has form [4]:

$$B_r = B_0\cos\theta w_1, \qquad B_\theta = B_0\sin\theta\frac{w_1 - w_2}{2},$$
$$E_\varphi = B_0\sin\theta\left(v - \frac{D}{2}\frac{\partial w_2}{\partial r}\right) \tag{2}$$

where

$$w_1(r,t) = \frac{1}{r^3}\int_0^r r'^2\, w_2(r',t)\,dr',$$

$$w_2(r,t) = \frac{1}{r\sqrt{\pi D}}\int_0^t \frac{dt'}{\sqrt{t-t'}}\int_0^\infty \left\{\exp\left[-\left(\frac{r+r'}{\alpha}\right)^2\right] - \exp\left[-\left(\frac{r-r'}{\alpha}\right)^2\right]\right\} g(r',t')\,dr', \tag{3}$$

$$\alpha = 2\sqrt{D(t-t')}, \qquad g(r,t) = r\frac{\partial v(r,t)}{\partial r} + 2v(r,t).$$

The velocity of a medium in an elastic wave is

$$v = \frac{r}{R}\left(\partial_t^2 f(\xi) + \frac{C_l}{r}\partial_t f(\xi)\right), \qquad \xi = \frac{C_l t - r}{R} + 1, \tag{4}$$
$$R \le r \le R + C_l t, \qquad 0 \le \xi \le C_l t$$

where $f(\xi)$ is the reduced elastic displacement potential. As the radius R of the spherical emitter, we choose the characteristic size of the earthquake focus or the radius of the destruction zone in the case of an underground explosion. Inside region $r \le R$ we define function $v(r,t)$ as follows:

$$v = \frac{r}{R}\left(\partial_t^2 f(\varsigma) + \frac{C_l}{r}\partial_t f(\varsigma)\right), \qquad \varsigma = \frac{C_l t}{R}. \tag{5}$$

Note that the form of the velocity distribution (5) at far distances from the epicenter (far zone) is not very significant.

Substituting (4) and (5) into (3) and integrating, we have

$$\begin{aligned} w_1 = \frac{1}{r^3}\int_0^t \Bigg\{ \Bigg[\Bigg(\frac{r^2 - R^2}{2} - \lambda(C_l t_1 + \lambda + R)\Bigg) g_+ + \lambda\big[(r+\lambda)\gamma_- + (r-\lambda)\gamma_+\big] + \\ + \sqrt{\frac{\lambda C_l t_1}{\pi}}\big[r h_+ - (2\lambda + R)h_-\big] + \eta(r - R - C_l t_1)\times \\ \times\left\{ (C_l t_1 + R)^2 - r^2 + 2\lambda\left[C_l t_1 + R + \lambda - (r+\lambda)\exp\frac{C_l t_1 + R - r}{\lambda}\right]\right\}\Bigg]\times \\ \times\frac{R}{C_l}\partial_t^3 f(t') + \Bigg[\frac{\alpha}{R\sqrt{\pi}}\left\{ rRh_+ - \left(r^2 + R^2 - \frac{\alpha^2}{2}\right)h_-\right\} - r^3 g_- - R^3 g_+\Bigg]\times \\ \times\left(\partial_t^2 f(t') + \frac{C_l}{R}\partial_t f(t')\right)\Bigg\} dt', \end{aligned} \tag{6}$$

$$w_2 = \int_0^t \Bigg\{ \Bigg[g_+ + \gamma_+ - \gamma_- - 2\eta(r - R - C_l t_1)\left(1 - \exp\frac{C_l t_1 - r + R}{\lambda}\right)\Bigg]\frac{R\partial_t^3 f(t')}{C_l r} - \\ - \frac{3}{R}\left(\frac{\alpha h_-}{r\sqrt{\pi}} + g_-\right)\left(\partial_t^2 f(t') + \frac{C_l}{R}\partial_t f(t')\right)\Bigg\} dt'.$$

The following notation is introduced in formulas (6):

$$\begin{aligned} g_\pm = \operatorname{erf}\frac{r+R}{\alpha} \pm \operatorname{erf}\frac{r-R}{\alpha}, \qquad \gamma_\pm = \operatorname{erfc}\left(\sqrt{\frac{C_l t_1}{\lambda}} + \frac{R \pm r}{\alpha}\right)\exp\frac{C_l t_1 \pm r - R}{\lambda}, \\ h_\pm = \exp\left[-\left(\frac{r+R}{\alpha}\right)^2\right] \pm \exp\left[-\left(\frac{r-R}{\alpha}\right)^2\right], \quad t_1 = t - t', \quad \lambda = \frac{D}{C_l}. \end{aligned} \tag{7}$$

Here erf (x) is the probability integral, erfc (x)= 1– erf (x), and η (x) is the unit function.

The nature of the given dependences is determined by the ratio between the size of the region covered by the diffusion process, $r_d \sim (Dt)^{1/2}$, and the distance $r_l = C_l t$

traveled by the elastic wave. Let us study the solutions for the far zone from the earthquake nidus ($r >> R,\ r >> r_d >> \lambda$) and time $t >> t^* = D/C_l^2$. Under these conditions we have $r >> \alpha$. Therefore, the arguments of the functions $g_\pm$, $h_\pm$, $\gamma_\pm$ are great. Using the asymptotics of the probability integrals for big values of the arguments, it is possible to obtain up to exponentially small terms of the order $\exp[-r^2/(4Dt)]$: $g_+ \approx 2,\ g_- \approx 0,\ \gamma_+ \approx 0,\ h_\pm \approx 0$. The behavior of a function γ_- depends on the sign of its argument.

Let us analyze solution (6) near the front of the elastic wave at $r \sim C_l t$. Let τ is the acoustic wave emission time. Then the source function becomes equal to zero at $t \geq \tau'$. Let us consider the times $t >> \tau$ when in integrals (6) the region of variation of variable $t' << t$ is most significant. Introduce the notation $\varepsilon = r - C_l t - R$. Then, if $|\varepsilon| << C_l t$, that $\gamma_- \approx 0$, since the argument of this function is much greater than unity. Moreover, the solution (2) for the wave front region ($\varepsilon \geq 0$) is simplified and takes form

$$B_r = -\frac{2B_0 R\lambda G(t,\varepsilon)}{r^2}\left(1+\frac{\lambda}{r}\right)\cos\theta, \qquad B_\theta = -\frac{B_0 R G(t,\varepsilon)}{r}\left(1+\frac{\lambda}{r}+\frac{\lambda^2}{r^2}\right)\sin\theta,$$
$$E_\varphi = \frac{B_0 R C_l G(t,\varepsilon)}{r}\left(1+\frac{\lambda}{r}\right)\sin\theta, \qquad G = \exp\left(-\frac{\varepsilon}{\lambda}\right)\int_0^t \exp\left(-\frac{t'}{t_*}\right)\partial_t^3 f(t')\,dt'. \tag{8}$$

Behind the wave front, i.e. when $\varepsilon < 0$, the solution has form

$$B_r = -\frac{2B_0 R\lambda}{r^2 C_l}\left\{\left(1+\frac{\lambda}{r}\right)G_1(t,\varepsilon) + \partial_t^2 f\left(-\frac{\varepsilon}{C_l}\right) + \frac{C_l}{\lambda}G_2(\varepsilon,r)\right\}\cos\theta,$$
$$B_\theta = -\frac{B_0 R}{r C_l}\left\{\left(1+\frac{\lambda}{r}+\frac{\lambda^2}{r^2}\right)G_1(t,\varepsilon) + \left(1+\frac{\lambda}{r}\right)\partial_t^2 f\left(-\frac{\varepsilon}{C_l}\right) + \frac{C_l}{r}G_2(\varepsilon,r)\right\}\sin\theta,$$
$$E_\varphi = \frac{B_0 R C_l}{r}\left\{\left(1+\frac{\lambda}{r}\right)\left[\partial_t^2 f\left(-\frac{\varepsilon}{C_l}\right) + G_1(t,\varepsilon)\right] + \frac{C_l}{r}\partial_t f\left(-\frac{\varepsilon}{C_l}\right)\right\}\sin\theta,$$
$$G_1 = \exp\left(-\frac{\varepsilon}{\lambda}\right)\int_{-\varepsilon/C_l}^{t} \exp\left(-\frac{t'}{t_*}\right)\partial_t^3 f(t')\,dt', \qquad G_2 = \partial_t f\left(-\frac{\varepsilon}{C_l}\right) + \frac{C_l}{r} f\left(-\frac{\varepsilon}{C_l}\right). \tag{9}$$

Formulas (9) relate to the seismic zone, and formulas (8) describe the structure of the EM wave, a precursor. It follows from (8) that in the precursor region the field decreases exponentially with a characteristic scale λ. This result can be explained as

follows. Since the precursor has a diffusion character, that in the stationary mode the characteristic diffusion propagation velocity $d_t\, r_d \sim (D/t)^{1/2}$ should be of the order of the velocity of the source of geomagnetic disturbances, i.e. longitudinal wave velocity C_l. It is not difficult to find from here the characteristic duration $t^* \sim D/C_l^2$ and spatial scale $\lambda \sim C_l t^* \sim D/C_l$ of the EM precursor.

At long distances ($\varepsilon \geq C_l t$), however, the approximations used above are no longer applicable. The perturbation attenuation law (8), in this case, is replaced by a sharper one: the field decreases proportionally $\exp[-r^2/(4Dt)]$ with distance.

Let us illustrate the above patterns by the example of a short single compression pulse. At long distances ($r >> R$), the expression for a longitudinal spherical wave is a combination of two half-waves: compression and rarefaction. Omitting the second term in (4) and taking into account that on the graph $v(t)$ the areas under the curve for the positive and negative phases should be equal in absolute value, we approximate the derivative $\partial_t^2 f(t)$ as follows

$$\partial_t^2 f = \begin{cases} v_1, & 0 < t < \tau_1; \\ -v_2, & \tau_1 < t < \tau_1 + \tau_2; \\ 0, & t < 0, \quad t > \tau_1 + \tau_2 \end{cases} \tag{10}$$

where $v_1 \tau_1 = v_2 \tau_2$. Then, using the δ-function we can write

$$\partial_t^3 f = v_1 \delta(0) - (v_1 + v_2)\,\delta(\tau_1) + v_2 \delta(\tau_1 + \tau_2). \tag{11}$$

Substituting now (10) and (11) into (9) and discarding small terms of order of λ/r, we have

$$\frac{B_\theta}{A} = \begin{cases} \exp\left(-\dfrac{\varepsilon}{\lambda}\right)\left[v_1 - (v_1 + v_2)\exp\left(-\dfrac{\tau_1}{t_*}\right) + v_2 \exp\left(-\dfrac{\tau_1 + \tau_2}{t_*}\right)\right], & \varepsilon \geq 0; \\ \exp\left(-\dfrac{\varepsilon}{\lambda}\right)\left[v_2 \exp\left(-\dfrac{\tau_1 + \tau_2}{t_*}\right) - (v_1 + v_2)\exp\left(-\dfrac{\tau_1}{t_*}\right)\right] + v_1, & 0 > \varepsilon \geq -C_l \tau_1; \\ v_2\left[\exp\left(-\dfrac{\varepsilon}{\lambda} - \dfrac{\tau_1 + \tau_2}{t_*}\right) - 1\right], & -C_l \tau_1 > \varepsilon; \end{cases} \tag{12}$$

$$E_\varphi = -B_\theta C_l; \qquad A = -B_0 R \sin\theta/(rC_l).$$

Dependence (12) is shown in Figs. 1 and 2. In the calculations, the parameters were chosen as follows:

$$C_l = 5 \text{ km/s}, \ \tau_1 = \tau_2 = 0.3 \text{ s}, \ v_1 = v_2 = 1 \text{ m/s}, \ B_0 = 10^{-5} \text{T},$$

$$\theta = \pi/2,\ R = 5\ \text{km},\ r = 20\ \text{km},\ \sigma = 10^{-1}\text{–}10^{-3}\ \text{S/m}$$

for curves 1–3 (in Figs. 1 and 2), respectively.

Let us estimate the amplitude of the magnetic field of the precursor B^* in the far zone. For $t^* >> \tau_1 + \tau_2$ (wavelength of the acoustic wave or medium conductivity is sufficiently small), one can use in formulas (12) the series expansion in a small parameter $\mu_0 \sigma C_l^2 (\tau_1 + \tau_2) << 1$ [4]. At this, after simplifications, we will have

$$B^* = -B_\theta(0) = B_0 R \mu_0^2 \sigma^2 C_l^3 \nu_1 \tau_1 (\tau_1 + \tau_2) \sin\theta/(2r). \qquad (13)$$

An analysis of formulas (12) shows that when passing from the precursor region ($\varepsilon > 0$) to the focal point ($\varepsilon < 0$), B_θ changes its sign, and the magnitude of the magnetic field reaches to its maximum amplitude

$$B_{\max} = B_\theta(-C_l \tau_1) = B_0 R \mu_0 \sigma C_l \nu_2 \tau_2 \sin\theta / r \qquad (14)$$

at $\varepsilon = -C_l \tau_1$. Expression (14) represents the amplitude of the main signal that occurs after the arrival of a seismic wave to the observation point, i.e. the amplitude of the induction seismomagnetic effect. From a comparison of (13) and (14), we can obtain

$$\frac{B^*}{B_{\max}} = \frac{\mu_0 \sigma C_l^2 \nu_1 \tau_1 (\tau_1 + \tau_2)}{2\nu_2 \tau_2} \sim \frac{l}{\lambda} = \frac{\tau_1 + \tau_2}{t_*} << 1 \qquad (15)$$

where $l = C_l (\tau_1 + \tau_2)$ is the acoustic wavelength, and λ is the precursor wavelength.

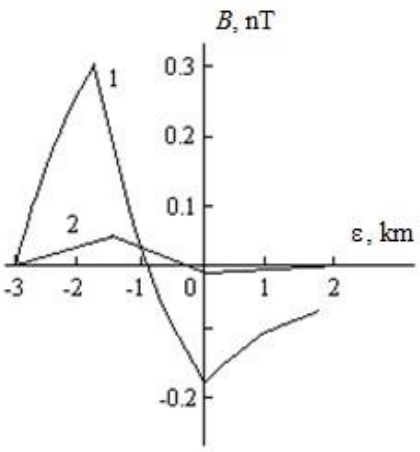

Fig. 1. Tangential component of magnetic disturbances in dependence on $\varepsilon = r - C_l t - R$; curves 1 and 2 correspond to the values $\sigma = 10^{-1}$ and 10^{-2} S/m, respectively.

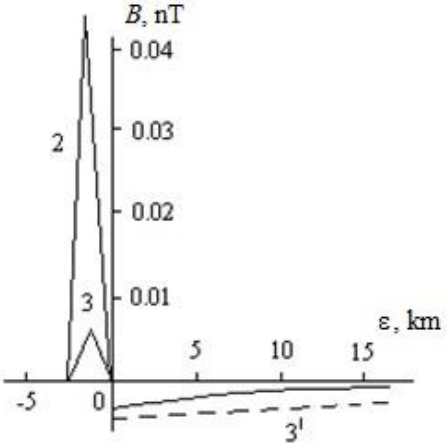

Fig. 2. Tangential component of magnetic disturbances in dependence on $\varepsilon = r - C_l t - R$; curves 2 and 3 correspond to the values $\sigma = 10^{-2}$ and 10^{-3} S/m, respectively.

Thus, the magnetic perturbations of the precursor and the main signal at their maxima have opposite polarities, and the amplitude of the precursor is much smaller. The case considered corresponds to the parameters of the problem corresponding to curve 3 in Fig. 2, where the dashed line (curve 3') shows the part of the graph related to the precursor and increased 100 times.

With increasing σ, the amplitude of the precursor increases, and its extent in space, $\lambda = D/C_l = (\mu_0 \sigma C_l)^{-1}$, decreases, and for small values of the conductivity σ of the medium $B^* \lambda^2 \approx \text{const}$.

In limit $\sigma \to \infty$ the following estimate holds:

$$B^* = \frac{B_0 R v_1}{r C_l} \sin\theta \sim B_0 \frac{v(r)}{C_l} \tag{16}$$

where $v(r) \sim R v_1 / r$ is the velocity amplitude. As can be seen from (16), B^* does not depend on σ. Since the magnetic field is frozen into the medium, we have $\lambda \to 0$. For the source region, in the considered limit, we have

$$B_{\max} = \frac{B_0 R v_2}{r C_l} \sin\theta . \tag{17}$$

Since $B^* / B_{\max} = v_1 / v_2$, the amplitudes (16) and (17) are approximately of the same order. However, the signals corresponding to them are still opposite in sign.

The results obtained above can be explained as follows. A seismic wave generates external currents with a density $\mathbf{j}_{cm} = \sigma[\mathbf{v}, \mathbf{B}_0]$. It can be shown that the effective magnetic moment $\mathbf{p}_m$ associated with currents $\mathbf{j}_{cm}$ is directed opposite to the field $\mathbf{B}_0$. Expressions (8) give the field of this moment taking into account the screening arising due to the skin effect. Assuming in (8) that $\sigma \to 0$, we obtain

$$B_r = -\frac{2 G_3 \lambda^2}{r^3} \cos\theta, \qquad B_\theta = -\frac{G_3 \lambda^2}{r^3} \sin\theta, \qquad G_3 = \frac{B_0 R}{C_l} \partial_t^2 f(t),$$

whence it is seen that $\mathbf{p}_m = -4\pi G_3 \lambda^2 \mathbf{B}_0 / (B_0 \mu_0)$. The minus sign here is due to the diamagnetic effect of a moving conducting medium. Consequently, the projections of magnetic disturbances at long distances from the epicenter are negative. For the same reason, the EM precursor signal is negative.

As shown in [4], a precursor feature is the perturbations' increasing as the front of the acoustic wave approaches the observation point (see also Figs. 1 and 2). Therefore, single EM pulses that are ahead of the acoustic wave by several seconds or even several minutes can hardly be interpreted as EM precursors of an earthquake. The origin of these signals, apparently, has a different nature. Despite the fact that the existence of EM precursors of seismic events is theoretically proven, experimental data on their observation are not yet reliable enough.

3. Manifestation of Seismic Effects in the Ionosphere in Near and Far Zones from the Nidus of Earthquake

Now, we will implement a phased approach to solving the problem. First, we consider the influence of an acoustic impulse caused by a surface wave caused by an earthquake in the atmosphere and the neutral component of the ionosphere near the source – epicenter (near zone), taking into account losses due to the weak electrical conductivity of the medium. At this, we will assume that for $\lambda_0 << z << z_0$ (z_0 is the height where the shock wave is formed, λ_0 is the size of the perturbed region), the vertical velocity of gas in the atmosphere will be described with sufficient accuracy by the linear approximation. At $z \sim z_0$ nonlinear mechanisms "turn on". Next, we consider the effect of wave perturbation in the neutral component on the ionized component of the ionospheric plasma. Then, we consider the nonlinear evolution of the perturbation in the neutral component propagating at ionospheric heights close to the horizontal plane in the far zone from the source, where the "high-frequency" acoustic oscillations decay due to the influence of dispersive effects and oscillations related to the IGW-branch begin to dominate. Next, we discuss the effect of such IGWs on the ionized component of the ionospheric plasma, as well as the effect of stochastic fluctuations of the wave field on the propagating wave.

To describe the movements of the neutral component, we consider the following set of equations of gas dynamics [15]:

$$\partial_t \rho' + \operatorname{div}\left[\rho_0(z)\mathbf{V}\right] = 0,$$

$$\rho_0(z)\left[\partial_t \mathbf{V} + (\mathbf{V}\nabla)\mathbf{V}\right] = -\nabla p' - \rho' g\,\mathbf{e}_z + \eta(z)\left[\tfrac{1}{3}\nabla \operatorname{div}\mathbf{V} + \nabla^2\mathbf{V}\right] + \varsigma(z)\nabla(\nabla\mathbf{V}), \quad (18)$$

$$\partial_t p' + \left(\mathbf{V}, \nabla p_0(z)\right) = -c^2\rho_0(z)\operatorname{div}\mathbf{V}$$

where the unperturbed values of the quantities that determine the wave field are indicated by the index "0", and the strokes indicate the perturbed values of the functions if their unperturbed values are zero. Functions without indices describe fields with unperturbed values equal to zero. In Eqs. (18) ρ is the density, p is the pressure for which unperturbed value $p_0(z) = \rho_0(z)c^2/\gamma = gH\rho_0(z)$ where $\gamma = C_p/C_v$, H is the scale height of the neutral atmosphere, $\eta(z) \approx 3c^2\rho_0(z)/2\gamma\nu_{nn}(z)$ is the dynamic viscosity coefficient, ν_{nn} is the collision frequency of neutral particles, and $\varsigma(z)$ is the kinematic viscosity coefficient. We further assume that the density of the unperturbed atmosphere and ionosphere is uniform with height z: $\rho_0(z) = \rho_0(0)\exp(-z/H)$.

Equations (18) do not take into account stochastic fluctuations of the fields, and we will introduce the corresponding terms further.

3.1. Near Earthquake Zone

To study the effects in the near earthquake zone, we assume that the fields are independent of the *y* coordinate, since it can be assumed that the disturbance in the surface wave is independent of *y*, and the properties of the medium change only in the *z*-axis direction. To describe an earthquake in the near zone, the function of horizontal coordinates and time was chosen in the form similar to that considered in [12], in axially symmetric form:

$$Z(r,t) = h(t) \times f(r/L), \tag{19}$$

and the vertical component of the displacement velocity of the earth's surface in form [14]

$$V_z\big|_{z=z(r,t)} = d_t h \times f(r,L) = V_0(t) \times f(r,L) \tag{20}$$

where L and $\max\{h(t)\}$ are the horizontal and vertical scales of the earthquake near the epicenter, respectively, $f(x)$ – is the dimensionless function normalized to unity, $\max\{f(x)\}=1$; functions $h(t)$ and $V_0(t)$ describe non-stationary character of motion of surface $Z(r,t)$. The form of the functions $V_0(t)$, $f(x)$ and $\eta(z)$ will be specified further. Since inequality $|h(t)| << L$ in real conditions is satisfied, the boundary condition on the $z = 0$ plane will have the form [14] $V_z\big|_{z=0} = V_0(t) \times f(r,L)$. Another boundary condition should correspond to asymptotics $z \to +\infty$; therefore, we can require that function $V_z(t,z,r)$ be a superposition of the waves $V_z(\omega,z,k)$ $V_z(\omega,z,k) \to 0$ at $z \to +\infty$ for $\eta \neq 0$), where $V_z(\omega,z,k)$ is a Fourier image of function $V_z(t,z,r)$ in t and its Fourier-Bessel image in r. The formulation of such a boundary condition ensures the flow of energy into the region $z = +\infty$. Note that formulas (19) and (20) are also valid for approximating the movements of the earth's surface caused by volcanic eruptions [4, 10], however, we do not touch upon this problem here.

Using the Fourier-Bessel transform in form

$$V_z(\omega,z,r) = \int_0^\infty k J_1(kr)\, V_r(\omega,z,k)\, dk,$$

$$\begin{bmatrix} V_z(\omega,z,r) \\ p'(\omega,z,r) \\ \rho'(\omega,z,r) \end{bmatrix} = \int_0^\infty k J_0(kr) \begin{bmatrix} V_z(\omega,z,k) \\ p'(\omega,z,k) \\ \rho'(\omega,z,k) \end{bmatrix} dk, \tag{21}$$

linearizing set (18) and eliminating ρ’ and p’ from (18), we obtain a set of ordinary second-order differential equations with variable coefficients [14]:

$$\left[\omega^2/c^2 - k^2 + i\delta(z)\left(\tfrac{4}{3}k^2 - d_z^2\right)\right]V_r = k\left[d_z - 1/\gamma H_1 - \tfrac{1}{3}i\,\delta(z)\,d_z\right]V_z, \qquad (22)$$

$$\left[d_z^2 - H^{-1}d_z + \omega^2/c^2 + i\,\delta(z)\left(\tfrac{4}{3}d_z^2 - k^2\right)\right]V_z = -k\left[d_z - (\gamma-1)/\gamma H_1 - \tfrac{1}{3}i\,\delta(z)\,d_z\right]V_r$$

where $\delta(z) = \omega\eta(z)/c^2\rho_0(z) = \omega/\omega_0(z) \approx 3\omega/2\gamma\nu_{nn}(z)$ is the dimensionless Knudsen number. In gas dynamics there is inequality $|\delta| << 1$, and we will further assume that δ is a small parameter.

Using nonlinear substitution, we introduce two new functions F and Ψ instead of V_z and V_r:

$$V_z = A\exp\left(z/2H + i\int_0^z F dz'\right), \qquad V_r = \left[\frac{k\left(iF - 1/\gamma H + 1/2H\right)}{\omega^2/c^2 - k^2} + \Psi\right]V_z \qquad (23)$$

where A = const. Boundary condition for $z = +\infty$ corresponds to condition Im $F \geq 0$ in (23). Functions F and Ψ satisfy some set of nonlinear equations [4]. Omitting the details, we write at once the results obtained at solving this nonlinear set for the acoustic branch of oscillations in the case of "small" heights z when

$$|\omega| >> c/2H > \left[g(\gamma-1)/\gamma H\right]^{1/2}, \qquad |z\delta/H| << 1, \qquad \int_0^z F dz' \approx F(z)z. \qquad (24)$$

For the vertical component of the velocity of neutral particles V_z, we obtain the following representation for the Fourier images:

$$V_z(\omega, z, r) \approx V_0(\omega)\exp(z/2H)\Phi_z(\omega, z, r), \qquad (25)$$

$$\Phi_z \approx \frac{i\,f(k_s)\Omega_1 \sin\chi\,\omega^2}{cR\left(\omega^2 - \omega_3^2\right)}\left(1 + \frac{ic}{R\,\varepsilon(\omega)}\right)\exp\left[i(R/c)\,\varepsilon(\omega)\right] \qquad (26)$$

where

$$\varepsilon(\omega) = \Omega_1\Omega_2,$$

$$\Omega_1 = \sqrt{\omega^2/(1 - 4i\delta/3) - \omega_1^2}, \qquad \Omega_2 = \sqrt{(\omega^2 - \omega_3^2)/(\omega^2 - \omega_2^2)},$$

$$\omega_1 = c/2H, \quad \omega_2 = \left[g(\gamma-1)/\gamma H\right]^{1/2}, \quad \omega_3 = z\omega_2/R, \quad R^2 = z^2 + r^2,$$

$$k_s = c^{-1}\omega\,\varepsilon(\omega)\cos\chi, \quad \chi = \arccos(r/R).$$

Further study depends on the specific form of the function $f(k)$. Let for earthquake

$$f(r/L) = \exp(-r^2/L^2). \qquad (27)$$

Then $f(k) = \pi L^2\exp(-k^2L^2/4)$ and the condition of a slow change of function

$f(k)$, which was used in (26), leads to bounding from above on the scale of the earthquake:

$$R^2 / L^2 >> \left| c^{-1} r \varepsilon(\omega) \cos\chi \right| = \left| k_s R \left[1 - (\omega_3^2 / \omega^2) \cos\chi \right] \right|$$

where $\left| k_s R \right| >> 1$. Now, we can obtain the expression for $V_r(\omega, z, r)$:

$$V_r(\omega, z, r) \approx V_0(z) \exp(z / 2H) (\partial_z - 1/\gamma H + 1/2H) \Phi_r(\omega, z, r) \qquad (28)$$

where

$$\Phi_r \approx -\Omega_2^{-1} R^{-1} \frac{k_s^2 f(k_s) \operatorname{tg}\chi}{\omega^2 / c^2 - k_s^2} \exp\left[i (R/c) \varepsilon(\omega) \right]. \qquad (29)$$

Expression (28) is valid when conditions (24) are satisfied, as well as the condition $\left| \sqrt{\phi(k_s) - \phi(k_p)} \right| >> 1$, $\phi(k) \approx kr + Fz$, $k_p = \omega / c$. When considering the acoustic disturbance in the far zone, where $\left| R c^{-1} \varepsilon(\omega) \right| >> 1$, the expressions for the Fourier images V_z and V_r take the following form:

$$V_z(\omega, z, r) \approx P R_0(\omega) / R, \qquad V_r(\omega, z, r) \approx P R_1(\omega) / R \qquad (30)$$

where

$$P = V_0(\omega) \exp\left[z / 2H + i (R/c) \varepsilon(\omega) \right], \qquad R_0(\omega) = \frac{-i f(k_s) \Omega_1 \sin\chi \, \omega^2}{c(\omega^2 - \omega_3^2)},$$

$$R_1(\omega) = \frac{-i k_s^2 f(k_s) \Omega_2^{-1} \operatorname{tg}\chi}{k_p^2 - k_s^2} \times \left(c^{-1} \varepsilon(\omega) \sin\chi + i/\gamma H - i/2H \right)$$

[compare with formulas (26), (29)]. Let us now use the continuity equation for perturbation of the electron density in the following form:

$$N_e'(r,t) = (2\pi)^{-1} i N_0(z) \cos\alpha \partial_z \int_{-\infty}^{\infty} \frac{d\omega}{\omega} V_{\|}(\omega, z, r) e^{i\omega t} -$$

$$-(2\pi R)^{-1} i N_0(z) \sin\alpha \partial_r \left\{ r \int_{-\infty}^{\infty} \frac{d\omega}{\omega} V_{\|}(\omega, z, r) e^{i\omega t} \right\} \qquad (31)$$

where $V_{\|} = \left| V \mathbf{H}_0 / H_0 \right|$ ($\mathbf{H}_0$ is the magnetic field), $\alpha = \pi/2 - I$, I is the magnetic inclination. Then we can obtain the approximate expression for the perturbation of electron density in the following form:

$$N'_e(t,z,r,\varphi) \approx (2\pi R)^{-1} i\, N_0(z) \cos\alpha \int_{-\infty}^{\infty} \frac{d\omega}{\omega} \Gamma(\omega,z,r) \times$$

$$\times \left[1/2H(z') + i\,\varepsilon(\omega,R)\sin\chi/c(z')\right] - \qquad (32)$$

$$- (2\pi R)^{-1} i N_0(z) \sin\alpha \int_{-\infty}^{\infty} \frac{d\omega}{\omega} \Gamma(\omega,z,r) \times i\,\varepsilon(\omega,R)\cos\chi/c(z')$$

where

$$\Gamma(\omega,z,R) = \mathrm{e}^{-i\omega t} V_0(\omega) \left[-R_0(\omega,R)\cos\alpha + R_1(\omega,R)\cos\varphi\cos\alpha\right] \times$$

$$\times \exp\left\{ \int_0^z dz'/2H(z') + i\int_0^R dR'\,\varepsilon(\omega,R')/c(R') \right\}$$

and φ is the angle between the planes $(\mathbf{z},\mathbf{H}_0)$ and $(\mathbf{z},\mathbf{V})$.

To obtain quantitative estimates of the magnitude of perturbations of the electron density in the ionosphere *F*-layer caused by non-stationary oscillations of the earth's surface as a result of an earthquake, we performed calculations in accordance with formula (32). At this, the following values of the basic ionospheric parameters were chosen: a) for heights $z < z'' = 100$ km – $c = 300$ ms^{-1}, $H = 6.7$ km, $\nu_{nn} = \nu_{nn}(z'')\exp\left[(z''-z)/H\right]$; b) for heights $z > z''$ the values of the ionospheric parameters were taken from the tables [16].

Calculations were performed for various spatial scales of the earthquake L in formula (27) for three types of approximation of the displacement velocity of the earth's surface:

$$V_0(t) = S_1 \beta_1^2\, t\, \exp(-\beta_1 t),$$

$$V_0(t) = 2S_2\, \Theta_1 \beta_2\, t\, \exp\Theta_1, \qquad \Theta_1 = 1 - \beta_2 t^2,$$

$$V_0(t) = \tfrac{1}{4} S_3\, \Theta_2 \beta_3^2\, t\, \exp\Theta_2, \qquad \Theta_2 = 2 - \beta_3 t.$$

These formulas describe various types of earthquakes. The first approximation corresponds to earthquakes, which lead to an increase or decrease of the level of the earth's surface with maximum amplitude S_1 at point $r = 0$. Two other approximations describe earthquakes accompanied by oscillations of the earth's surface with different relaxation times. The results of calculations for different values of parameters $\beta_1, \beta_2, \beta_3$ are shown in Fig. 3.

Fig. 4a shows the results obtained for different spatial scales of the earthquake. One can see that the ionosphere response is quasiperiodic in nature with oscillation periods about 40–80 s, moreover, the amplitude of the response substantially depends both on the temporal nature of the initial disturbance of the earth's surface $V_0(t)$ and

on its spatial scale L. This can be explained by the filtering properties of the atmosphere with a frequency band from the acoustic cutoff frequency ω_a to the upper frequency, which is defined by the viscosity of the atmosphere.

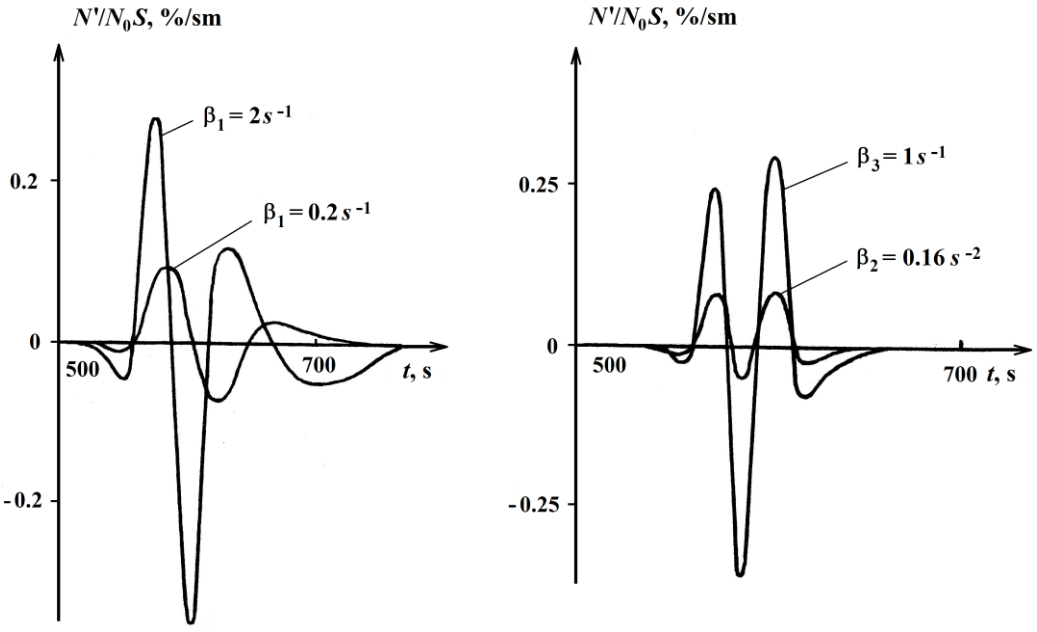

Fig. 3. Dependence of nature of response of the ionosphere on the type of earthquake; L=10 km, z =190 km, r =70 km, φ = 0°, α=10°.

The dependence of the ionospheric response on the distance to the epicenter is shown in Fig. 4b. One can see that the amplitude of the perturbation decreases and the quasi-period increases with distance.

The results obtained are in qualitative agreement with the results obtained in [4] and [12], some differences are related to the fact that in our analysis we take into account weak nonlinearity, which is weakly manifested at the heights considered here and small distances from the epicenter. It should be noted, in particular, that we have considered the region of the ionosphere above the earthquake nidus zone and near this zone. In the far zone, other mechanisms of excitation of perturbations of electron density being switched on as we will show further.

3.2. Far Earthquake Zone

In this case, we will also be based on nonlinear equations of gas dynamics (18). However, now we should take into account that spatial dispersion leads to damping of the oscillations of the acoustic branch with propagation of the disturbances over big distances, that results in a shift of the spectral maximum to a lower-frequency region. Along with decreasing the role of sources such as an acoustic pulse, the role of a surface Rayleigh wave as a source of IGWs grows with distance relatively [13, 14].

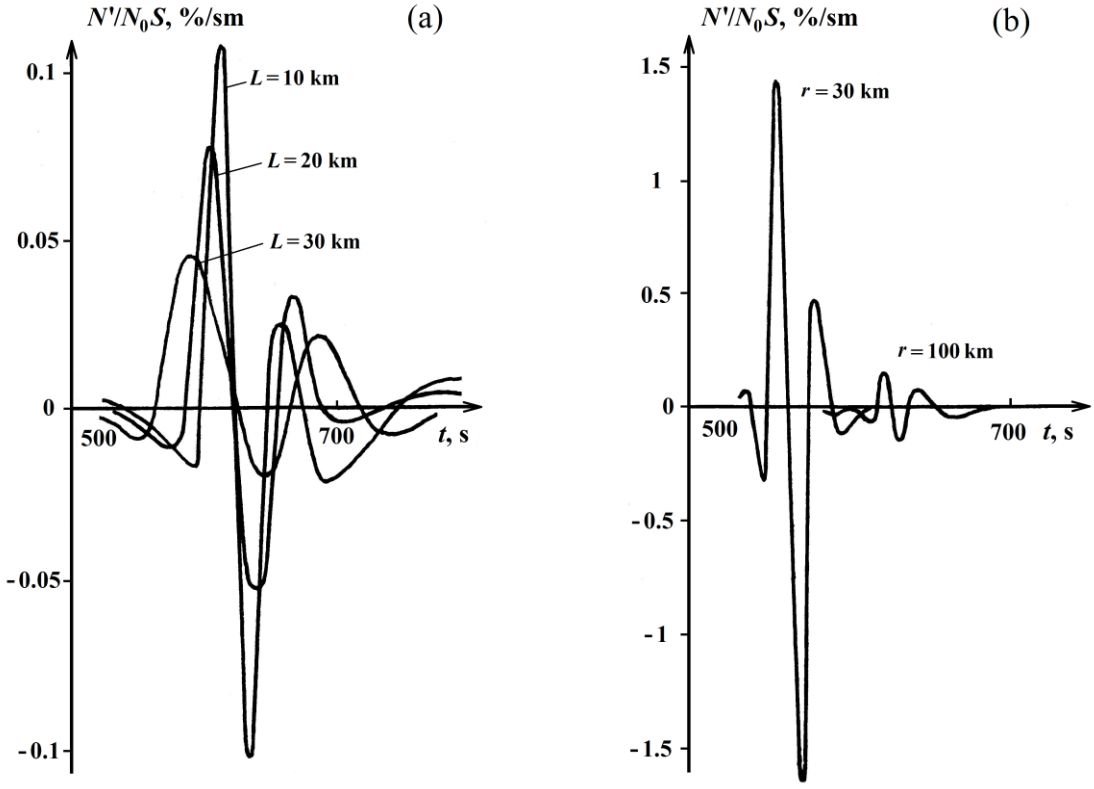

Fig. 4. Dependence of nature of response of the ionosphere on spatial scale of the earthquake and distance from the epicenter for φ = 0°, α=10°: (a) – β_1=0.2 s^{-1}, z =190 km, r =70 km; (b) – β_1=2 s^{-1}, z =180 km, L=10 km.

The first boundary condition approximating a surface Rayleigh wave at large distances from the epicenter is chosen in the following form:

$$V_z\big|_{z=0} = d_t Z(r',t), \qquad Z(r',t) = h(t)\exp\left[-(r')^2/L^2\right] \tag{33}$$

where

$$(r')^2 = \xi^2 + y^2, \qquad \xi = x - v_R\, t,$$

v_R is the velocity of the Rayleigh wave. Thus, we will consider the problem in the coordinate system associated with the Rayleigh wave. Another boundary condition for Eqs. (18) which corresponds to condition $z \to +\infty$ will be the same as in the problem for the near zone (see above), but for function $V_z(t,z,\xi,y)$. The Rayleigh wave (33) leads to the formation of a wave going upward with an amplitude growing with height, which is associated with an exponential decrease of density: $\rho_0(z) = \rho_0(0)\exp(-z/H)$ (see above). Nonlinear effects begin to manifest themselves at the heights of the ionosphere *F*-region, when a nonlinear solitary IGW is formed under the action of the going upword wave excited by the surface Rayleigh wave [15].

Taking into account the geometry of the problem, we assume that $k_x^2 >> k_\perp^2$,

$|Hk_x| << 1$, i.e. for nonlinear solitary waves propagating at angles close to the horizontal plane, the Boussinesq approximation is valid. Then, the set of Eqs. (18), taking into account weak nonlinearity for the velocity of neutral particles $u(t,r',z) = V(t,r,z)\big|_{x=\xi+vt}$ at $\partial_z = 0$, can be reduced to one fifth-order equation – the Belashov-Karpman (BK) equation obtained in [17] taking into account the term describing the dissipative effects of the viscous type [15, 18]:

$$\partial_t u + \frac{2\gamma-1}{\gamma^2} u_z \partial_\xi u - \sigma \partial_\xi^2 u + 2\frac{(\gamma-2)^2}{\gamma^2} vH \partial_\xi^3 \left[u + \frac{(\gamma-2)^2}{2\gamma^2} \varepsilon H^2 \partial_\xi^2 u \right] = \frac{v}{2} \int_{-\infty}^{\xi} \partial_y^2 u \, d\xi \tag{34}$$

where $\gamma = C_p / C_v$, $\varepsilon = -v / v_{\min}^{ph}$, $v_{\min}^{ph}$ is the minimum phase velocity of linear oscillations, coefficient σ describes viscosity:

$$\sigma = (\rho_0 / 2\rho)\left(c_\infty^2 - c_0^2\right)\tau \int_0^\infty \mu \phi(\mu)\, d\mu = (2\rho_0)^{-1}\left[\tfrac{4}{3}\eta + \varsigma + \gamma\left(\frac{1}{C_v} - \frac{1}{C_p} \right) \right]$$

where c_∞ and c_0 are the velocities of the "high-frequency" and "low-frequency" sound [19], respectively.

Considering the solitary waves traveling at the near-to-horizontal angles, the continuity equation for the electron density N_e in the *F*-layer can be written in the following form [15, 17]:

$$\partial_t N_e = \partial_z \left[(\partial_z N_e + N_e / 2H_i) D_0 \, e^{z/H_i} - u_z \left(1 - e^{-\upsilon t'}\right) \sin I \cos I \right] - \beta N_e + Q \tag{35}$$

where $D_0 \exp(z/H_i) = D_\alpha \sin^2 I$, D_α is the ambipolar diffusion coefficient, $\beta = \beta_0 (-Pz / H_i)$ and Q are, respectively, the recombination rate and the ion production rate; $t' = t - t_0$ where t_0 is the moment of the start of the neutral component's perturbation; H_i is the scale height for ions.

Approximating the profile of electron density at height z by $N_e = N_{e0} \exp(z/H_i)$, $N_{e0} = N_e\big|_{z=0}$, we obtain the solution of Eq. (35) in form [20, 21]

$$N_e(u,t) = N_e(u,t_0) \exp\left[\Im(u,t) \right], \qquad \Im(u,t) = \int_{t_0}^{t} g(u,t)\, dt \tag{36}$$

where

$$g(u,t) = C - \left(1/H_i + 1/2H\right) f(u,t), \qquad C = 3a/H_i^2 - \beta(1-q),$$

$$f(u,t) = uc \exp(z/2H)\left(1 - e^{-\upsilon t'}\right) \sin I \cos I, \qquad q = Q/\beta N_e, \qquad a = D_\alpha \sin^2 I.$$

Function u in solution (36) satisfies Eq. (34).

As shown [15, 17, 18, 21], in the case $\varepsilon << -1$ the solutions of Eq. (34) for $\sigma = 0$ have form of the algebraic solitons of the Kadomtsev-Petviashvili equation, therefore in this case the integral in right-hand side of solution (36) can be calculated analytically [due to cumbersomeness, we do not present here the analytical form of the functional $\Im(u,t)$]. Solution (36), describing the traveling ionospheric disturbance (TID), has also the form of the algebraic soliton [17, 20, 21] (see Fig. 5). If, however, $\varepsilon \to -1$ or $\varepsilon << -1$ at $\sigma \neq 0$ it is necessary to use numerical integration of Eq. (34), since for these cases its analytical solutions are unknown. The results of numerical integration of Eqs. (34), (36) at $\sigma = 0$ for typical values of the parameters of the *F*-layer and soliton solution of Eq. (34), describing the disturbances travelling with the velocities ~ 200 ms^{-1}, were presented in our papers and book [13, 15, 17, 20, 21] (an example of these results is shown in Fig. 6). In these works, it was shown that for $N' = \{[N(u,t) - N(0,t)]/N(0,t)\} \times 100\%$ function $N'(u,t)$ in this case has a wave character with an increasing steepness of the leading front like a shock wave. At this, both the phase shift of the TID relative to the IGW phase (about 0.5–5 min) and the relaxation effect in the recovery of density N' after passing of the IGW soliton are noted. These effects increase with a decrease of ε, which determines the value of spatial dispersion.

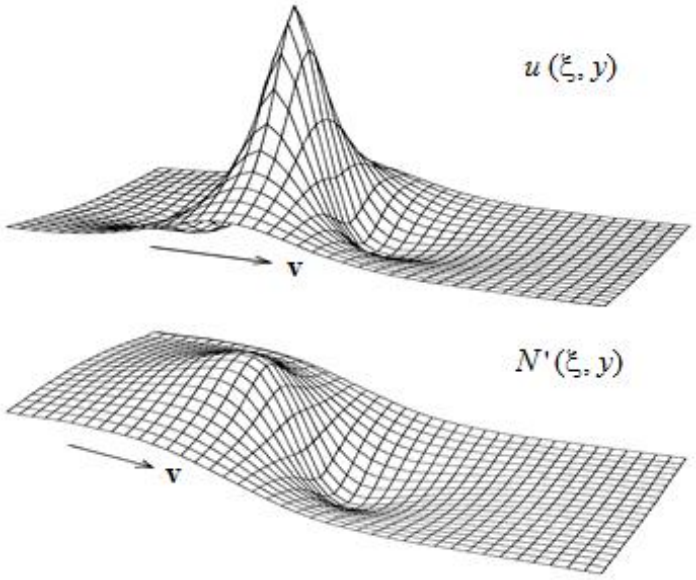

Fig. 5. IGW disturbance of soliton type (u) at $\varepsilon = -12$ and the corresponding disturbance of the electron density $N' = \{[N(u,t) - N(0,t)]/N(0,t)\} \times 100\%$.

The case $\sigma \neq 0$ was studied in detail in our works [18, 22] where it was shown that taking the dissipative term into account leads to the exponential decay of the perturbation with decreasing its amplitude with decrement $\Gamma(t) \sim \sigma$. In this case, the effects of violation of the structure and symmetry of the IGW soliton along with the relaxation effect in the recovering N' are also observed.

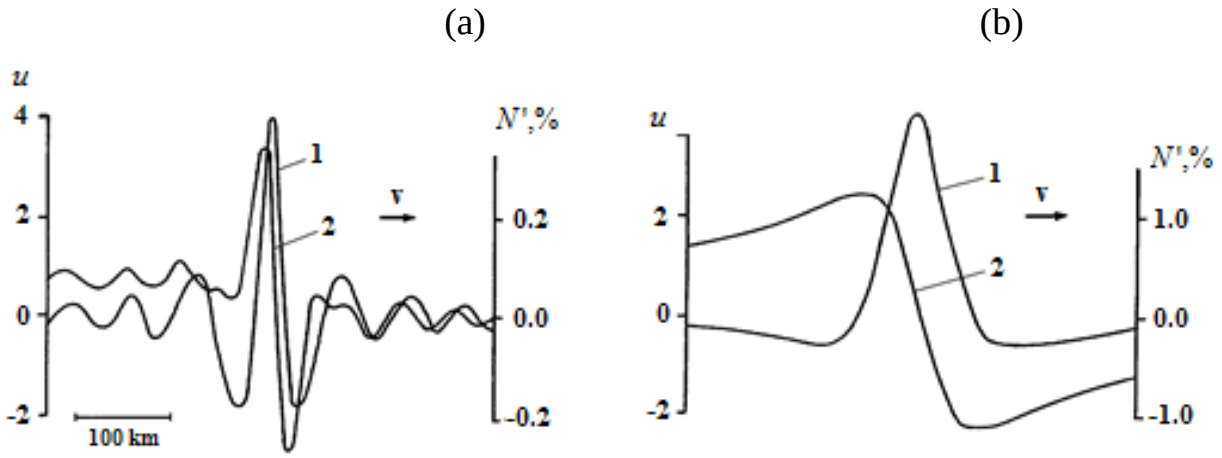

Fig. 6. Profiles of the perturbations at $y = 0$: 1 – IGW, 2 – TID (N') for $\varepsilon = -1.2$ (a) and $\varepsilon = -12$ (b).

When taking into account the influence of stochastic fluctuations of the wave field, which almost always occur at ionospheric heights, on the evolution of the TID excited by the Rayleigh wave, Eq. (34) should be supplemented by term $\kappa(t, r', z)$ describing such fluctuations. The case of low-frequency stochastic fluctuations, when $\kappa = \kappa(t)$ and $\varepsilon = 0$ in Eq. (34), was studied in detail analytically in [23] and all the results obtained there can be easily transferred to our Eq. (34) with term $\kappa = \kappa(t)$. So, even small stochastic fluctuations of the wave field lead to the scattering of the disturbance during its propagation, while the scattering IGW soliton of Eq. (34) acquires the wave structure.

However, in the case when $\kappa = \kappa(t, r', z)$ an analytical study of this process becomes extremely difficult [24] and we used numerical simulation for this purpose. The results obtained were qualitatively similar to the case $\kappa = \kappa(t)$ [15]: damping of the oscillating solutions and their destruction with time are also observed. The obtained estimates showed that in the *F*-layer it is practically impossible to distinguish the ionospheric response excited by the surface Rayleigh wave at distances from the epicenter $r >> 12–13\ L$.

4. Discussion and Conclusion

The analysis, presented in Sect. 2, shows that an EM precursor appears in front of the seismic wave front in a conducting medium, and the precursor amplitude exponentially decreases with distance, with a characteristic scale $\lambda = (\mu_0 \sigma C_l)^{-1}$. For the upper layer of sedimentary rocks, $\lambda \sim 1–100$ km, therefore, the precursor can be ahead of the elastic wave by no more than a few seconds. In the case of a single compression pulse, the precursor signal is negative. At this, its amplitude increases with time up to the moment of arrival of the seismic wave. At distances of the order of tens of kilometers from the epicenter, the precursor amplitude can reach values

from several pT to nT for magnetic disturbances and from several nV/m to μV/m for electric ones, depending on the medium conductivity and seismic wave parameters. With increasing conductivity of the medium, the precursor amplitude increases, and its characteristic size λ decreases. All these effects are very general in nature and can be observed not only in the ground, but also in sea water [4], for example, at propagation of tsunami waves.

As for the seismic effects in the ionosphere in near and far zones from the nidus of earthquake (Sect. 3), note that the study of the multidimensional case, taking into account all significant factors (weak nonlinearity and dispersion, dissipation, and stochastic fluctuations of the wave field), allows us to obtain more accurate results for both the near and far zones of the earthquake epicenter. Thus, for a few types of approximation of the displacement velocity of the earth's surface it was shown that in the near zone of the earthquake the ionosphere response is quasiperiodic with oscillation periods about 40–80 s, and the amplitude of the response depends on temporal and spatial scales of the initial disturbance of the earth's surface. At this, the amplitude decreases and the quasi-period increases with distance. On big distances it is necessary to take into account that spatial dispersion leads to damping of the oscillations of the acoustic branch with propagation and a shift of the spectral maximum to a lower-frequency region is observed. In this case, the surface Rayleigh wave excites the perturbation of the neutral component of the atmosphere in form of a solitary IGW which is a source of the solitary TID at heights of the *F*-layer of the ionosphere. Nonlinear effects lead to increasing steepness of the TID leading front, and dissipation leads to the exponential decay of the perturbation with decreasing its amplitude. A presence of even small stochastic fluctuations of the wave field leads to scattering of the disturbances during its propagation, and the solitary IGW and TID pulses acquire the wave structure. On big distances from the earthquake epicenter, damping of the oscillating disturbances and their destruction with time are observed.

In conclusion, we have presented the results of study of displaying of seismic activity in variations of both the EM field and the basic ionospheric characteristics. We have showed that considering of the 3D case with a due account of the effects of weak nonlinearity, dispersion and dissipation in medium enables to obtain more accurate results for both the near and far zones of the earthquake epicenter. In study of the seismic response in the EM field, it was confirmed that a precursor arises ahead the front of seismic wave, and it was shown that its amplitude depends on the medium conductivity and the parameters of the wave. Regarding the response at ionospheric heights, the seismo-ionospheric post-effects were studied, that is of great interest, in particular, for a better understanding of relationships in the system "solid Earth – atmosphere – ionosphere" and for identification of seismically caused oscillations in the spectrum of the ionospheric fluctuations, etc. The effect of the acoustic impulse caused by the Rayleigh wave on the ionosphere's neutral component near the epicenter was also considered, and formation of the solitary IGWs and the TIDs, which are caused by it, at heights of the F-layer in the far zone was studied. The results obtained

are in good agreement with the results of our radiophysical experiments during seismic events at the Russia Far East region [25-27].
The work is performed according to the Russian Government Program of Competitive Growth of Kazan Federal University. This work was also supported by the Shota Rustaveli National Science Foundation (SRNF), grant no. FR17 252.

References

1. Belov S.V., Migunov S.V., Sobolev G.A. *Magnetic effects accompanying strong Kamchatkan earthquakes*, Geomagn. and Aeronom., 1974, V. 14(3), pp. 380-382.
2. Sorokin V.M., Fedorovich G.M. *Propagation of short-period waves in the ionosphere*, Radiophys. Quantum Electron., 1982, V. 25, pp. 352-362. https://doi.org/10.1007/BF01035307.
3. Surkov V.V. *Propagation of geomagnetic pulsations in the E-layer of the ionosphere*, Geomagn. and Aeronom., 1990, V. 30(1), pp. 121-126.
4. Belashov V.Yu. *Comprehensive studies of seismic activity in the natural electromagnetic field and ionosphere of the Earth*, Research Report, Lab. Seismology and Petrophysics, 2000a, V. 3(3), pp. 7-26. Magadan: NEISRI FEB RAS [in Russian].
5. Surkov V.V. *Perturbation of an external magnetic field by a longitudinal acoustic wave*. Magnetohydrodynamics, 1989a, V. 25, pp. 145-148.
6. Surkov V.V. *Geomagnetic perturbations in a stratified medium, caused by propagation of a longitudinal spherical wave*, J. Appl. Mech. Tech. Phys., 1989b, V. 30(5), pp. 687-696. https://doi.org/10.1007/BF00851410.
7. Guglielmi A.V. *Magnetic structure of the front of an elastic wave*. Izvestiya, Phys. Solid Earth, 1991, V. 4, pp. 53-58.
8. Surkov V.V. *Electromagnetic precursor of seismic wave*, Geomagn. and Aeronom., 1997, V. 37(6), pp. 155-160. https://doi.org/10.1007/BF01035223.
9. Golitsin G.S., Klyatskin V.I. *Atmospheric oscillations caused by movements of Earth's surface*, Izv., Atm. Ocean. Physics, 1967, V. 3(10), pp. 1044–1052.
10. Pavlov V.A. *Effect of earthquakes and volcanic eruptions on the ionospheric plasma*, Radiophys. Quantum Electron., 1979, V. 22, pp. 10-23. https://doi.org/10.1007/BF01035223.
11. Pavlov V.A. *Acoustic impulse above the epicenter of the earthquake*, Geomagn. and Aeronom., 1986, V. 26(5), pp. 807-815.
12. Doilnitsina E.G., Drobyazko I.N., Pavlov V.A. *On influence of earthquakes on the electron density in the F layer of the ionosphere*, Geomagn. and Aeronom., 1981, V. 24(7), pp. 783-793.
13. Belashov V.Yu. *The earthquake-induced IGW's in the ionosphere F layer*. Proc. IX Intern. Wroclaw Symp. on EMC, Wroclaw, Poland, 1988, V. 1, p. 227. New York: IEEE, Inc.

14. Belashov V.Yu. *Seismogenic perturbations at heights of ionosphere F layer*. Intern. Workshop on Seismo Electromagnetics (IWSE-97), Tokyo, Japan, 1997a, pp. 225-233. Tokyo: NASDA.
15. Belashov V.Yu., Vladimirov S.V. *Solitary Waves in Dispersive Complex Media. Theory, Simulation, Applications*. Springer-Verlag, Berlin-Heidelberg-New York-Tokyo, 2005.
16. Alpert Ya.L., Gurevich A.V., Pitaevsky L.P. *Space Physics with Artifical Satellites*. NY: Consultants Bureau, 1965.
17. Belashov V.Yu. *Dynamics of nonlinear internal gravitational waves at heights of the ionospheric F-region*, Geomagn. and Aeronom., 1990, V. 30(4), pp. 637-641.
18. Karpman V.I., Belashov V.Yu. *Dynamics of two-dimensional solitons in weakly dispersive media*, Phys. Lett. A. , 1991, V. 154(3/4), pp. 131-139.
19. Karpman V.I. *Non-linear waves in dispersive media*, Pergamon. Oxford, 1975
20. Belashov V.Yu. *Solitary electron density waves induced by the IGW's solitons in the ionosphere*, Proc. Intern. Symp. on EMC, Nagoya, Japan, 1989, V. 1, p. 228. New York: IEEE, Inc.
21. Belashov V.Yu., Belashova E.S., Kharshiladze O.A. *Nonlinear wave structures of the soliton and vortex types in complex continuous media: theory, simulation, applications*, Lecture Notes of TICMI, Tbilisi Intern. Centre of Mathematics and Informatics, Tbilisi, Georgia, 2017, V. 18.
22. Belashov V.Yu. *Dissipation's effect on structure and evolution of nonlinear waves and solitons in plasma*, Proc. XI Intern. Wroclaw Symp. on EMC, Wroclaw, Poland, 1992, V. 2, p. 591. New York: IEEE, Inc.
23. Belashov V.Yu. *Dynamics of KP equation solitons in media with low-frequency wave field stochastic fluctuations*, Phys. Lett. A., 1995a, V. 197, pp. 282-286.
24. Belashov V.Yu. *Dynamics of nonlinear waves and solitons in plasma with wave field stochastic fluctuations*, Workshop on Theory and Observ. of Nonlin. Processes in the Near-Earth Envir., Warsaw, Poland, 1995b, V. 4.1. Warsaw, Space Research Center.
25. Belashov V.Yu., Kabanov V.V. *Experimental Study of Ionospheric Effects Related to Seismic Activity on the Russian North East Station Network*, XXV General Assembly of URSI, Lille, France, 1996, V. 677. Lille: URSI.
26. Belashov V.Yu. *Some Results of Common Analysis of Ionospheric and Seismic Data Obtained in the Periods of Seismic Activity on the Russian North East Station Network*, Intern. Workshop on Seismo Electromagnetics (IWSE-97), Tokyo, Japan, 1997b, pp. 234-238. Tokyo: NASDA.
27. Belashov V.Yu. *Comprehensive studies of seismic activity in the natural electromagnetic field and ionosphere of the Earth*, Research Report, Lab. Seismology and Petrophysics, 2000b, V. 3(3), pp. 43-55, NEISRI FEB RAS, Magadan [in Russian].